Available online at www.sciencedirect.com
SCIENCE DIRECT®

Journal of the European Ceramic Society 23 (2003) 585–594
www.elsevier.com/locate/jeurceramsoc

Corrosion of silicon nitride materials in acidic and basic solutions and under hydrothermal conditions

M. Herrmann[a,*], J. Schilm[a], G. Michael[a], J. Meinhardt[b], R. Flegler[b]

[a]*Fraunhofer-Institut für keramische Technologien und Sinterwerkstoffe, Winterbergstrasse 28, Dresden D-01277, Germany*
[b]*Fraunhofer-Institut für Silikatforschung, Würzburg, Germany*

Received 4 October 2001; received in revised form 6 August 2002; accepted 19 August 2002

Abstract

Silicon nitride ceramics with different amounts and compositons of the grain boundary phases are produced by gas pressure sintering and the corrosion behaviour was analysed in acids, bases and under hydrothermal conditions. The investigation shows, that the corrosion is strongly affected by the SiO_2 content in the grain boundary and the amount of the additives. The results indicate that the grains and the thin films between the grains are very stable in acids and bases but solves partially under hydrothermal conditions. The corrosion behaviour of the investigated materials with a relatively stable grain boundary phase in acids can be described by the same kinetic laws as those used to describe the corrosion of glasses. An interfacial reaction is assumed to be rate-controlling. The less stable material with Y_2O_3/Al_2O_3 additives can be described by the corrosion behaviour of oxide nitride glasses only at the beginning. For higher corrosion depths, the formation of protective barriers consisting of a hydrated SiO_2 network is assumed to occur.

Keywords: Corrosion; Hydrothermal corrosion; Kinetics; Si_3N_4

1. Introduction

Silicon nitride-based ceramics are promising engineering materials for application under corrosive and wear conditions due to their hardness, mechanical strength and good corrosion resistance at room and elevated temperatures. However, use of silicon nitride materials in hot acids is often limited by degradation of the materials. This is the impetus for current efforts to improve the corrosion behaviour of silicon nitride materials. It was shown[1–4] that the materials exhibit nearly no degradation in acids (HCl, H_2SO_4 and HNO_3) at room temperature, but the grain boundaries of the silicon nitride materials dissolve in hot acids. The MgO-containing materials show better corrosion resistance than the Y_2O_3/Al_2O_3-containing materials. The stability in highly concentrated acids is much greater than in moderately concentrated acidic solutions;[1–4] the reasons for this behaviour are not clear. Therefore, we investigated the corrosion behaviour of Si_3N_4 ceramics with different grain boundary compositions.

2. Experimental

Silicon nitride ceramics of different compositions (see Table 1) were prepared from Si_3N_4 [Baysinid ST (Bayer AG) SN E10 (UBE)], Al_2O_3 (AKP50), Y_2O_3 (HCST grade fine) and MgO (Merck) powders. The powders were mixed for 4 h in a planetary ball mill (agate bowls and balls). The materials were cold-isostatically pressed into bars (20×20×60 mm) at 200 MPa and gas-pressure sintered at 1800 °C for 3 h under a nitrogen pressure of 30 bar to a density of 99.9% of theoretical density. The materials were then cut and ground into bending bars. Some samples were polished before being tested. Additionally, oxide nitride glasses were prepared by melting the oxides and AlN (HCST grade) in BN crucibles at 1700 °C in a furnace with tungsten heating elements (see Table 2).

All samples were cleaned by ultrasonic treatment in water, acetone and subsequently ethanol before

* Corresponding author.
E-mail address: herrmann@ikts.fhg.de (M. Herrmann).

0955-2219/03/$ - see front matter
PII: S0955-2219(02)00303-5

Table 1
Compositions and properties of the investigated materials

Material	Additive vol%	Kind	SiO_2 in GB (mass%)	σ_0 (MPa)
MgAlSi 1	7.2	$MgAl_2O_4/SiO_2$	53	660
MgAl 1	5.9	$MgAl_2O_4$	45	801
MgAl 2	6.6	$MgAl_2O_4$	36	700
MgAl 3	8.4	$MgAl_2O_4$	29	940
YalMg 1	5.2	$MgAl_2O_4/Y_20_3$	52	830
YAlMg2 [1)]	7.2	$MgAl_2O_4/Y_20_3$	36	820
YAl 1 [1)]	10.9	Y_20_3/Al_2O_3	20	920

SiO_2 in GB—SiO_2 content in the grain boundary phase 1 with Baysinid powder.

Table 2
Compositions of the investigated glasses

	Mol%				HV_3	K_C
	Al_2O_3	Y_2O_3	SiO_2	Si_3N_4		
GLAY 2	30	20	47	3	855	1.5
GLAY 3	10	15	72	3	778	1.3
GLAY 4	30	30	37	3	923	1.3
GLAY 5	20	5	72	3	759	1.7
GLAY 6	25	20	55	0	834	1.3
GLAY 7	25	20	50	5		
GLAY 8	25	20	45	10		

undergoing corrosion testing. The materials were tested in 1 N and 2 N H_2SO_4 and in 1 N NaOH up to 130 °C and in distilled water up to 210 °C under pressure. The reaction vessels and sample holders were made of Teflon. The acidic and basic solutions were stirred during the corrosion tests. The samples were rotated (300 RPM) during the hydrothermal corrosion tests. The solutions were changed after 50–100 h. The ratio of the sample surface to the solution volume was lower than 5×10^{-3} m^{-1}. Therefore, the concentrations of solved components in the solutions were far from the corresponding equilibrium concentrations. After corrosion the strength, the weight loss and the thickness of the corroded layer was measured for the samples.

The surfaces of the materials were analysed using SEM and FESEM. Cross-sections were analysed using light microscopy and SEM.

Additionally, the corrosion behaviour of different oxide nitride glasses was tested to quantify the corrosion resistance of the grain boundary phase. Thin plates of glass were suspended from Pt wire in a Teflon reaction vessel. After different periods of time the solution was analysed (ICP-AES) and the samples cleaned in a US bath to remove surface corrosion layers, weighed and subjected to further corrosion. In a second set-up, the glass samples were not ultrasonically cleaned after the different periods of corrosion.

To determine whether or not the grain boundary phase forms a three-dimensional skeleton even at very low additives contents, the dihedral angles of the compositions YAl 1 and YAlMg 1 were measured on polished cross-sections (see Fig. 1a and b) and the mean of 50 measurements was calculated.

3. Results

3.1. Stability in H_2SO_4

The results of investigations are given in Table 3 and in Figs. 1 to 5. With decreasing amount of sintering additives, the corrosion rate in H_2SO_4 at 90 °C was found to decrease very rapidly (see Fig. 2). Analysis of corroded polished samples indicated that mainly the grain boundary phase in the triple junctions was attacked, whereas the grains and the thin inter-grain-boundary layers showed no signs of corrosion. Even after corrosion of the grain boundary phase up to a depth of about 1 mm from the surface, no reaction at the thin grain boundary layers was observed (see Fig. 1).

Table 3
Corrosion resistance of the sintered silicon nitride ceramics (corrosion constants were determined by regression using the following equations: $at+bt^{0.5}=\Delta m$ and $a+bt=\Delta m$, with Δm in mg/cm^2 and t in h)

Material	GB (vol.%)	σ_0 (MPa)	$\sigma_{(res.700\ h)}$, (MPa)	Corrosion depth (μm^2)	$at+bt^{0.5}=\Delta m$			$a+bt=\Delta m$		
					R^2	a (mg /(hcm^2))	b (mg /(h$^{0.5}$cm^2))	R^2	a (mg /cm^2)	b (mg /(hcm^2))
MgAl 1	2.7	801	720	<5	0.995	$5\cdot10^{-6}$	$1.5\cdot10^{-3}$	0.993	0.011	$4.72\cdot10^{-5}$
MgAl 2	3.6	700	650	<10	0.998	$6\cdot10^{-5}$	$2.5\cdot10^{-3}$	0.998	0.018	$1.27\cdot10^{-4}$
MgAl 3	5.4	940	660	450	0.991	$5\cdot10^{-3}$	0.2	0.975	1.2	0.01
YAL 1	10.9	920	470[a]	850						
YALMg2	5.2	820	780	<5	0.955	$1.5\cdot10^{-6}$	$2.1\cdot10^{-3}$	0.998	0.015	$7.5\cdot10^{-5}$

GB, grain boundary phase.
[a] After 300 h.

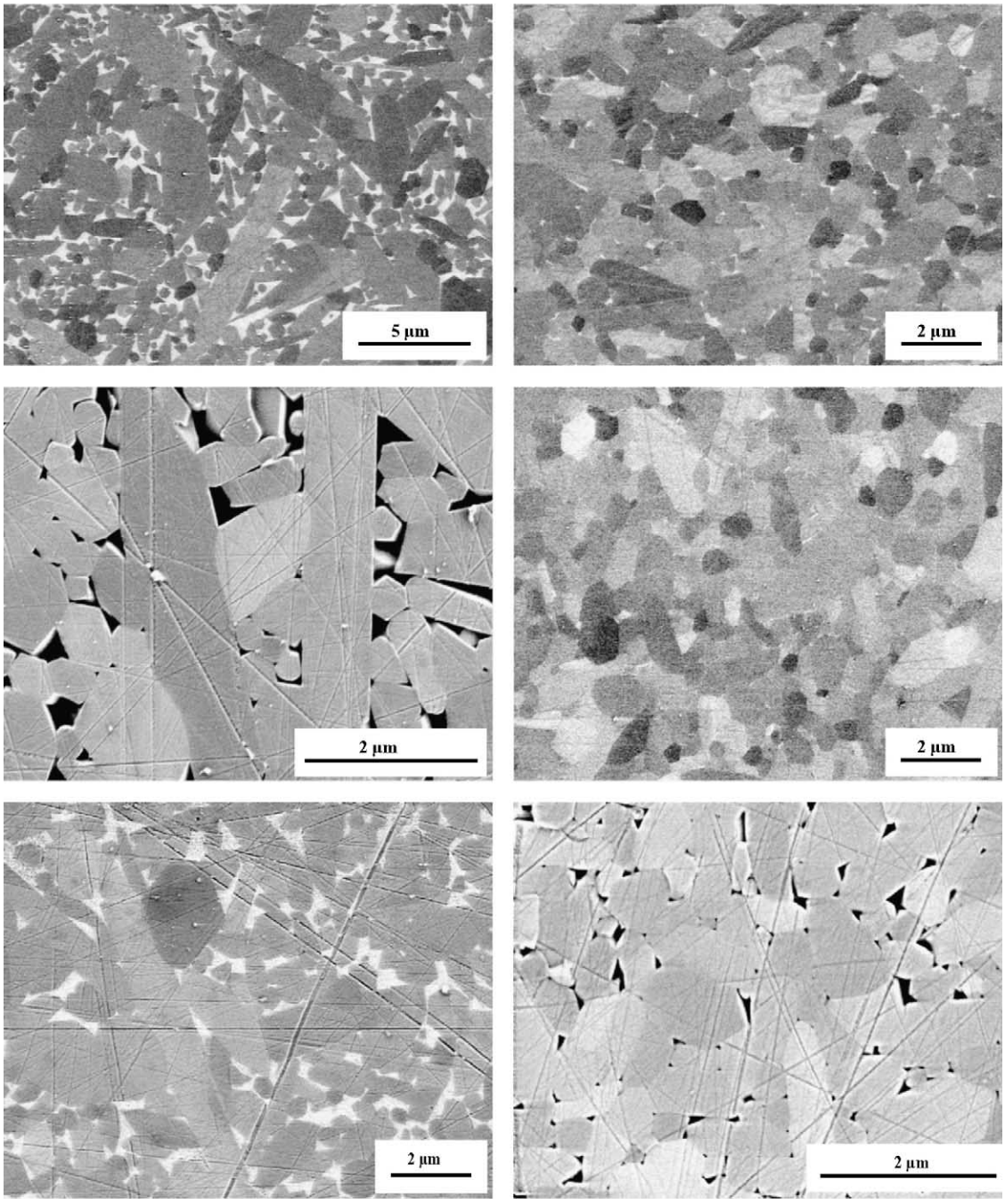

Fig. 1. SEM micrographs of the materials YAl 1 (a, c, e) and YAlMg (b, d, f): (a, b) uncorroded surfaces; (c, d) surfaces after 200 h in 1 N H_2SO_4 at 90 °C, and (e, f) surfaces after 50 h in 1 N NaOH at 90 °C.

The kinetics of the corrosion process, of the materials exhibiting relative stability in acidic, could be described by the two equation types

$$\Delta m = at + bt^{0.5} \quad (1)$$

or

$$\Delta m = a + bt \quad (2)$$

(see Table 3), where Δm is the specific weight loss, t is the time and a and b are constants. The first equation is often used for describing the corrosion of glasses,[5] whereas the second indicates a linear dependence on time, e.g. an interfacial reaction with some deviations at the beginning caused by the different corrosion behaviour of the surface. The materials with high corrosion rates (YAl 1) could not be described by a simple equation involving the shrinking core models.[6,7] After a few hours the corrosion rate of these materials strongly

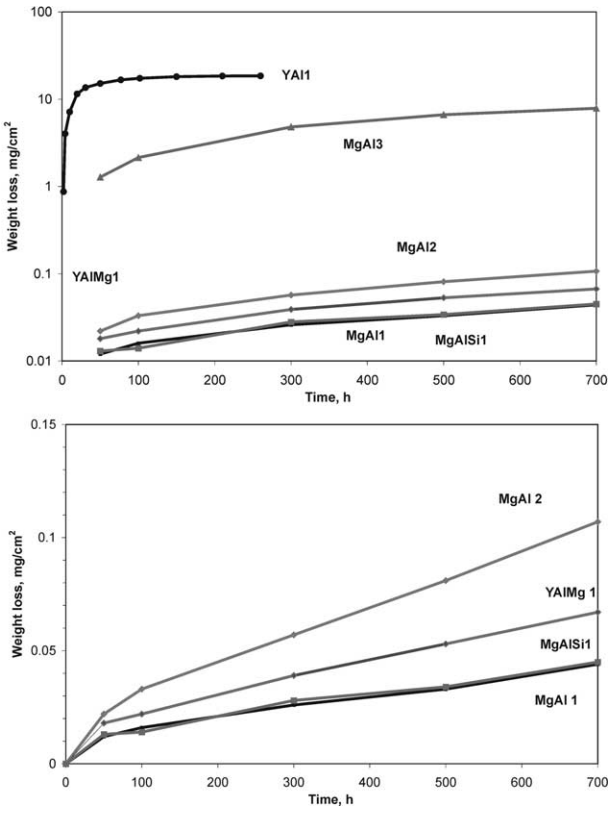

Fig. 2. Dependence of the weight loss on the corrosion time in 1 N H_2SO_4 at 90 °C: (a) on a logarithmic scale and (b) linear scale for stable materials.

decreased, indicating the existence of passivation mechanisms (see Figs. 2 and 4).

The residual strength of the materials after corrosion in acids is given in Tables 3 and 4. Even the materials in which the corrosion depth was about 850 μm (YAl 1) showed a strength as high as 450 MPa. This and the high mechanical stability of the corroded layer (no spalling of the corroded layer) were indicative of the low degree of chemical attack of the grains and the thin grain boundary films between adjacent grains (see Fig. 1).

The kinetics of corrosion for the prepared oxide nitride glasses in 2 N H_2SO_4 showed a linear dependence on time. Periodic ultrasonic cleaning increased the weight gain during corrosion (see Fig. 3). The concentration ratio of YAl to Si in the solution corresponded to the ratio of these elements in the glasses; i.e. solution of these glasses took place homogeneously. The corrosion rate was shown to depend strongly on the SiO_2 content in the glass samples (see Figs. 3 and 5). The lower the SiO_2 content the higher the corrosion rate.

Slightly different behaviour was shown by glass GLAY3, which is characterised by micro-immiscibilities of SiO_2. FESEM analysis of the corroded polished section showed that the small SiO_2-rich precipitates had a drastically lower corrosion rate than the matrix did (see Fig. 6). This is a evident behaviour because of the higher stability of SiO_2 against acide.

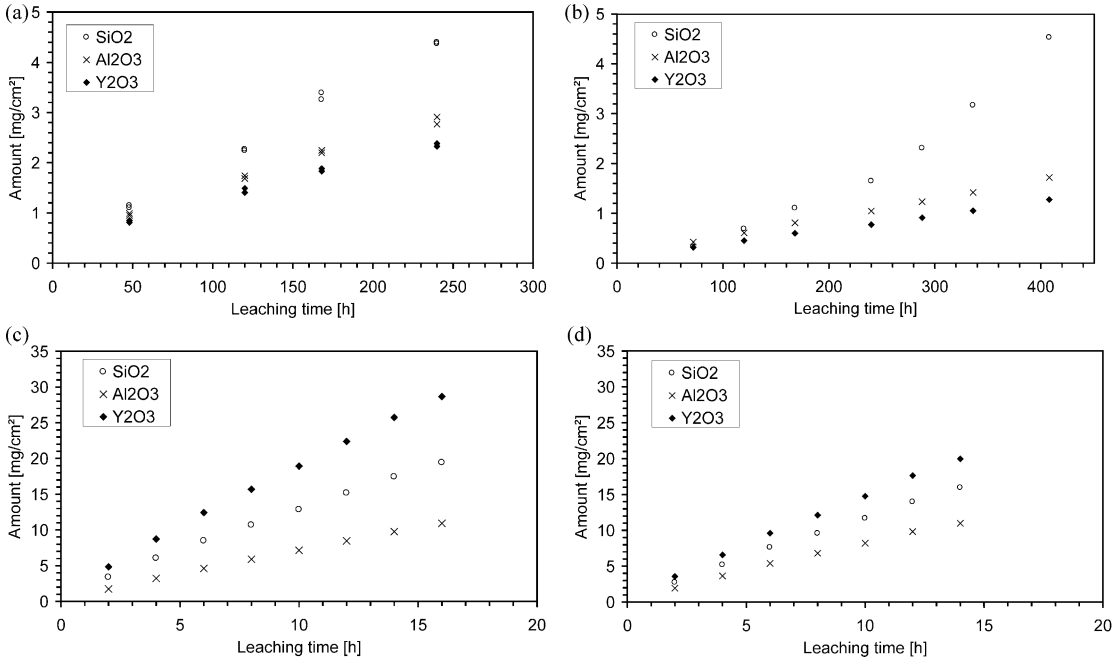

Fig. 3. Dependence of the leached amount of components on time for glasses GLAY5 (a and b) and GLAY 6 (c and d) (leaching conditions: 90 °C, 2 N H_2SO_4; a and c with periodic ultrasonic treatment; b and d no periodic ultrasonic treatment).

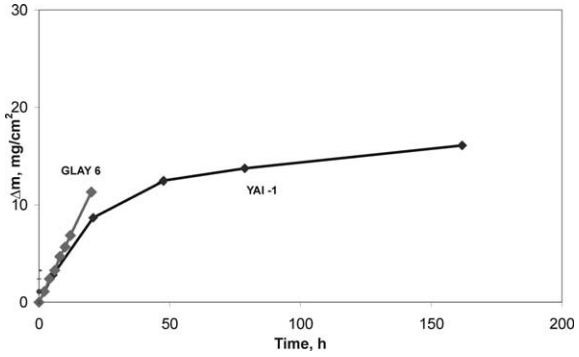

Fig. 4. Comparison of the corrosion behaviour (corrosion conditions: 2 N H_2SO_4, 90 °C) of material YAl 1 and glass GLAY 6 for a composition corresponding to the composition of the grain boundary phase (corrosion of GLAY 6—without periodic ultrasonic treatment).

3.2. Stability in HF

Even at room temperature, the 20%-HF solution attacked the silicon nitride materials (see Table 4 and Figs. 7 and 8). Analysis of the surfaces of the corroded samples showed that the HF solution attacked both the Si_3N_4 grains and the grain boundary phase. The corrosion resistance of the material that was more stable in H_2SO_4 was lower in HF (see Fig. 7).

3.3. Stability in NaOH

The weight loss and the residual strength as a function of time are given in Figs. 9 and 10 and in Table 4. The different materials did not demonstrate such extreme differences in weight loss, corrosion depth and residual strength as those materials that underwent corrosion in 1 N H_2SO_4 did (see Table 4). The greatest depth of corrosion observed after 200 h was only 30 μm. For the YAl 1 materials, the corrosion rate showed a linear dependence on time, whereas for the YAlMg 1 material, the corrosion rate decreased with time.

The different grain boundary phases behaved differently during corrosion in 1 N NaOH. The grain boundary phase of the material stable in acids, YAlMg 1, showed more degradation in NaOH than the grain boundary of the material unstable in acids, YAl 1, did (see Fig. 1). Also in this case, the grains and the thin films between adjacent Si_3N_4 grains showed no evidence of corrosion attack (see Fig. 1).

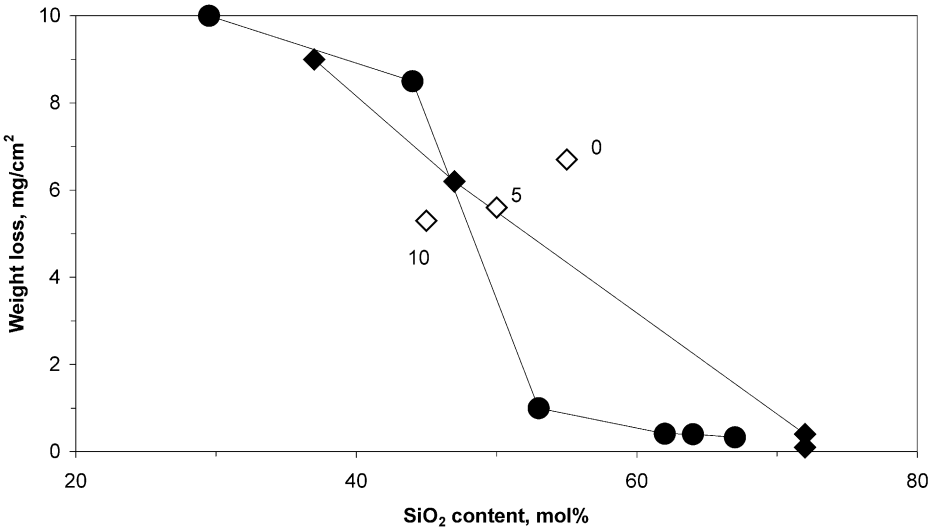

Fig. 5. Dependence of the weight loss on the SiO_2 content of the glasses (◆, glasses with 3 mol% Si_3N_4, ◇, glasses with changing concentration Si_3N_4 mol% Si_3N_4 are indicated) after 3 h in 1 N H_2SO_4 at 90 °C. and weight loss of Si_3N_4 materials (Y_2O_3/AlO_3 additives) (●) after corrosion in H_2SO_4 at 60 °C (200 h) as a function of the SiO_2 content in the grain boundary phase (according to references.[11,12]

Table 4
Strength, residual strength $\sigma\ (R)_{4b}$, weight loss Δm and thickness of the corrosion layer for materials YAl1 and YalMg1 (200 h corrosion)

Sample	Strength σ_{4b} (MPa)	1N NaOH (130 °C)			20% HF (20 °C)			1 N H_2SO_4 (boiling)			Hydrothermal corrosion (200 °C)		
		Δm (mgcm^2)	D (μm)	$\sigma\ (R)_{4b}$ (MPa)	Δm (mg cm^2)	D (μm)	$\sigma\ (R)_{4b}$ (MPa)	Δm (mg cm^2)	D (μm)	$\sigma\ (R)_{4b}$ (MPa)	Δm, (mg cm^2)	D (μm)	$\sigma\ (R)_{4b}$ (MPa)
YAl-1	920±50	0.05	<5	840±30	−0.4	20	440±10	−20.02	200	425±45	−0.19	<5	770±60
YAlMg2	820±100	0.17	30	740±30	−11	260	275±7	−0.35	<5	720±60	−0.31	15	715±45

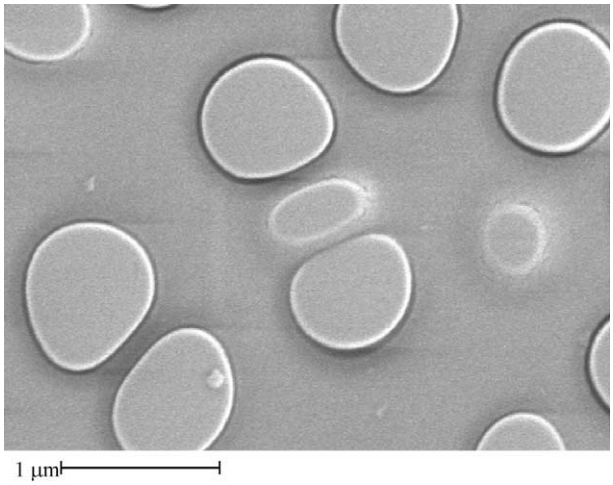

Fig. 6. SEM micrograph of the polished surface of the oxide nitride glass GLAY 3 after 2 h corrosion in 1 N H_2SO_4 at 90 °C.

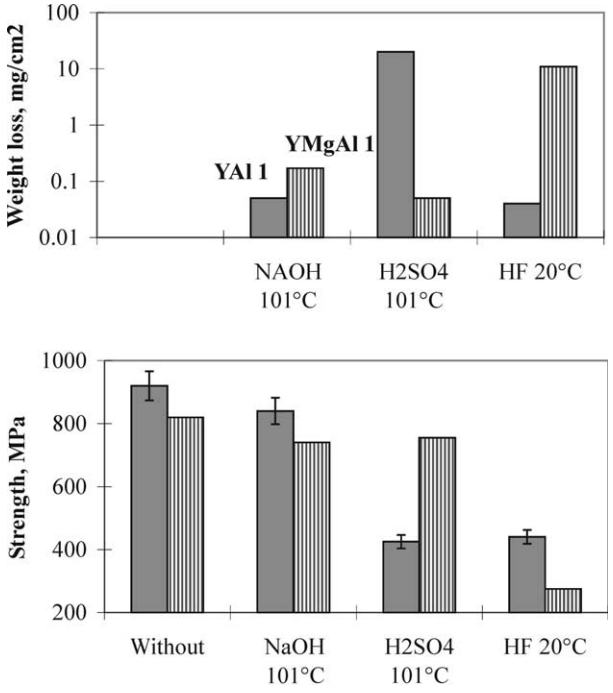

Fig. 7. Weight loss and residual strength for materials YAlMg 2 and YAl1 after 200 h corrosion in 20% HF (20 °C), in boiling 1 N H_2SO_4 and 1 N NaOH.

Corrosion of the oxide nitride glasses in 1 N NaOH at 90 °C was found to depend linearly on time, but the corrosion rate was found to be much lower than in acids under similar conditions. Analysis of the concentration of the elements in the solution showed that mainly the network former SiO_2 was solved (see Fig. 10). The corrosion rate was shown to depend on the SiO_2 content in the glass samples. The lower the SiO_2 content the lower the corrosion rate.

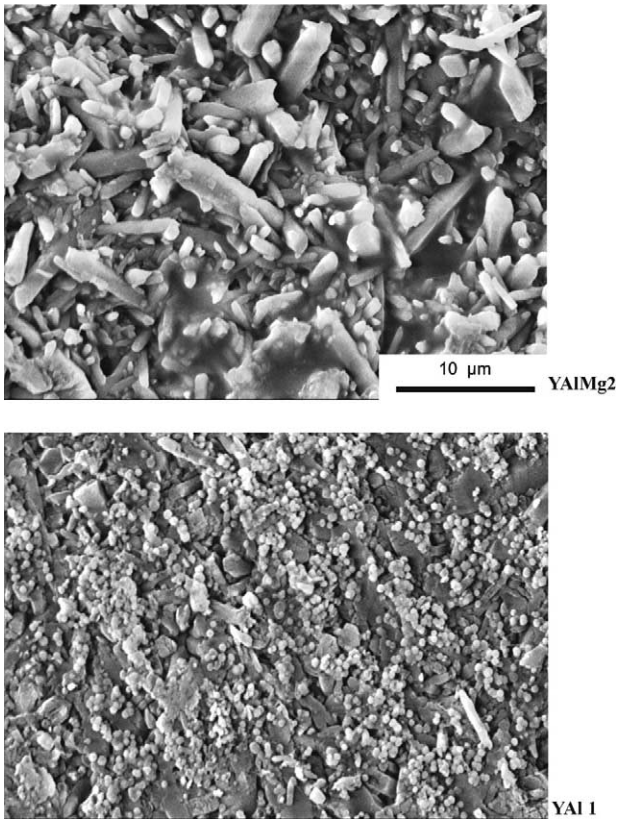

Fig. 8. SEM micrograph of materials YAl 1 and YAlMg 2 after 200 h corrosion in 20% HF at 20 °C.

3.4. Stability under hydrothermal conditions

The results of hydrothermal corrosion measurements are given in Table 4 and Figs. 11 and 12. Materials containing only $MgAl_2O_4$ (MgAl 1–3) as a sintering additive showed much lower corrosion resistance than materials containing both Y_2O_3 and $MgAl_2O_4$ or Y_2O_3 and Al_2O_3. The corrosion layer thickness for samples MgAl 1–3 after 250 h at 210 °C ranged from 50 µm (MgAl 3) to 120 µm (MgAl 2). For sample YAl 1, a corroded layer thickness of less than 5 µm was found. YAlMg 1 and YAl 1 showed similar behaviours. The surfaces of the corroded samples showed that under these corrosion conditions, both Si_3N_4 and the grain boundary phase solved. Therefore, the corroded layer was unstable and thicker corrosion layers could easily be removed (see Fig. 12). The weight losses during corrosion depended linearly on time.

4. Discussion

The experimental results show that the corrosion behaviour of silicon nitride ceramics depends mainly on the amount and composition of the grain boundary phase. To determine whether or not the grain boundary phase forms a three-dimensional skeleton even when its

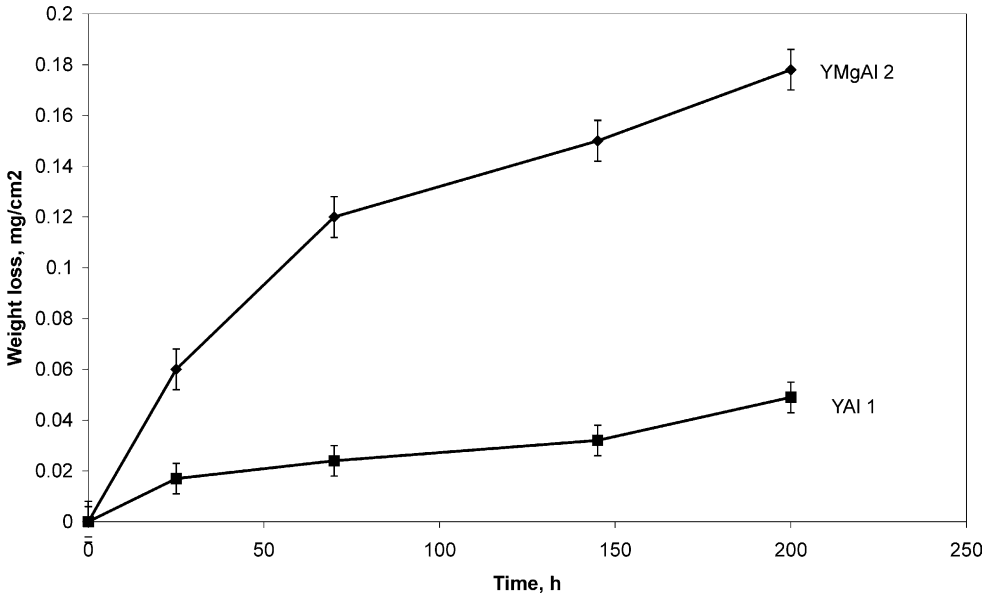

Fig. 9. Weight loss of Si_3N_4 ceramics Yal-1 and YAl Mg 2 in boiling 1 N NaOH as a function of the time.

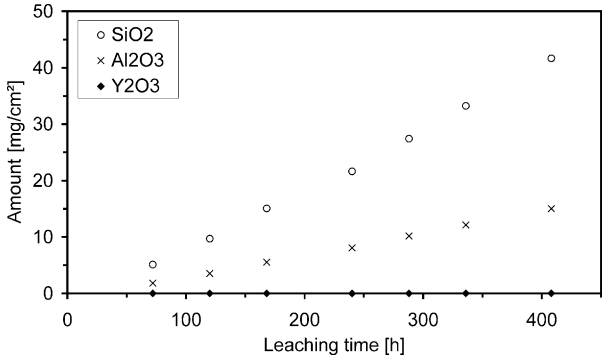

Fig. 10. Dependence of the leached amount of the components in the solution on time (leaching conditions: 90 °C, 1 N NaOH, no periodic ultrasonic treatment) for glass GLAY 6.

content is very low, the dihedral angles of the compositions YAl 1 and YAlMg 1 were measured on polished cross-sections (see Fig. 1a and b). The determined mean angles, 35±8° (YAl 1) and 37±7 ° (YAlMg 1), were far from the critical values (60° for less than 1 vol.% and approximately 95° for 10 vol.% grain boundary phase, corresponding to the angles at which a change in the grain boundary from continuous skeleton to discrete segregation takes place[8]). Therefore, one must assume that a three-dimensional grain boundary phase skeleton exists in the materials, even at a low additive content. Therefore changes in the corrosion stability cannot be directly connected with a change in the distribution of the grain boundary phase.

The grains and the thin films between the grains are not attacked by the solutions during corrosion in acids (excluding HF) and bases at least up to 130 °C (see Fig. 1). The reason for the different corrosion rates of the grain boundary films and the triple junctions seems to be connected with the different compositions of these two regions. TEM investigations and theoretical models[9,10] indicate that the thin films are richer in SiO_2 and Si_3N_4. The consequence of this stability is that the corrosion layer is stable up to a layer thickness of several hundred micrometers. This also explains the relatively high strength of the corroded material (similar to that of RBSN). In HF, the SiO_2-rich compounds are unstable due to the ability of HF in contradiction to other acids to solve SiO_2. Therefore HF dissolves both grains and the thin grain boundary films, and, the materials with SiO_2-rich grain boundary phases are less stable than the YAl 1 material is. Additionally, YF_3 has a low solubility and can form a passivating layer.

The corrosion behaviour of the investigated oxide nitride glasses and previous investigations[11,12] suggest that the SiO_2 content in the grain boundary phase is a main parameter governing the corrosion behaviour of the material. Materials with a high SiO_2 content in the grain boundary phase are more stable in acids and less stable in bases. Likewise, materials with a low SiO_2 content in the grain boundary phase are stable in bases and under hydrothermal conditions, but less stable in acids. This behaviour is more pronounced in materials with a higher amount of grain boundary phase.

The influence of the Y/Al ratio on the corrosion resistance is not investigated in detail up to now. But existing results [6,12,13] suggest that the influence of the Y/Al ratio is less pronounced than the influence of the SiO_2 content.

The corrosion kinetics of the Si_3N_4 materials with high stability in acids can be described by the same laws that are used for glasses. In these cases (YMgAl1, MgAl 2), interfacial control of the dissolution of the grain bound-

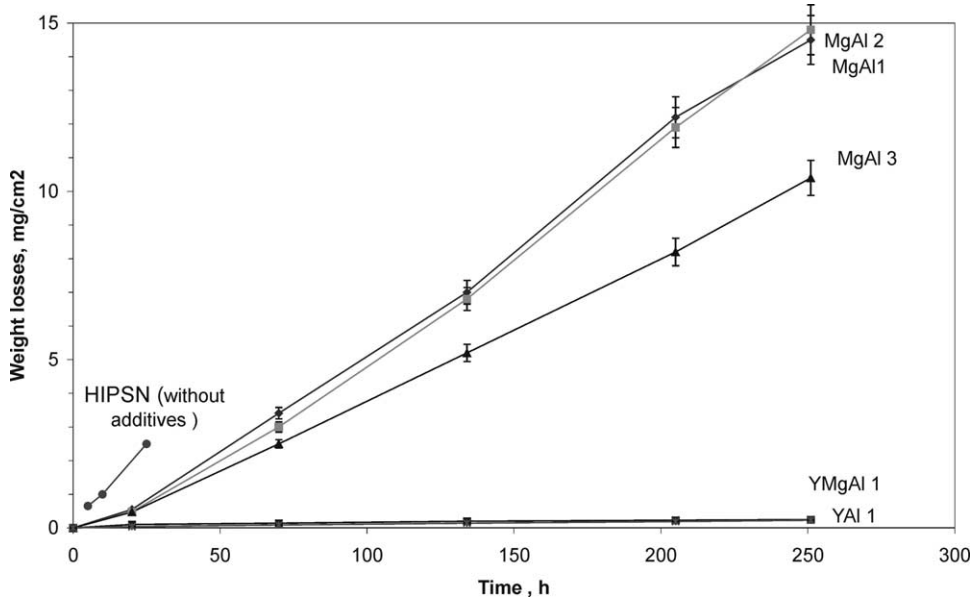

Fig. 11. Weight losses of materials during hydrothermal corrosion at 210 °C (data for HIP SN taken from Ref. 1).

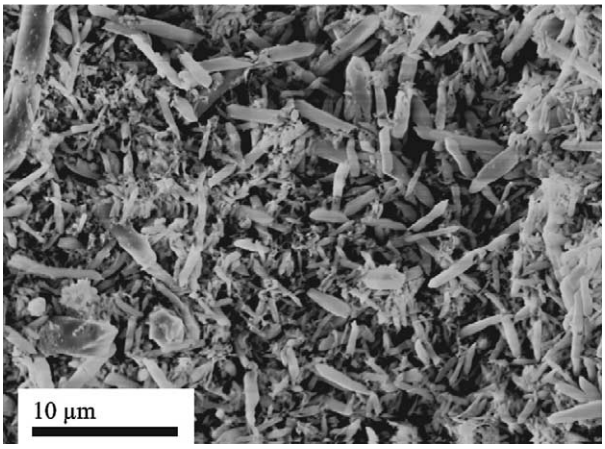

Fig. 12. SEM micrograph of material MgAl 2 after hydrothermal corrosion at 210 °C.

ary is likely. However, the corrosion depth after several hundred hours is less then a few micrometers. The corrosion kinetics of materials with low-corrosion-resistant YAl 1 can only be described using the data of the oxide nitride glasses with similar compositions in the grain boundary phase (GLAY-6) in the initial state (see Fig. 4). The corrosion rate of material YAL-1 is very similar to that of glass GLAY 6 (experimental set-up without periodic ultrasonic treatment of the surface) up to a corrosion time of 10–15 h. After 10–15 h the corrosion rate of YAl 1 is significantly lowered. This reduction cannot be explained by the shrinking core model. Attempts to explain this drop in the corrosion rate by diffusion control were also unsuccessful.[7] Therefore, it must be assumed that a protective corrosion layer is formed.

To make this process clearer, knowledge of the corrosion of glasses can be used. Corrosion of glass in acids is featured by leaching of the network modifier (in our case Y, Mg and particulary Al) and formation of a hydrated glass network in the first step. Shematically this can be illustrated by the following reaction:

$$\equiv (\mathrm{Si-O})_n\text{–M} + n\mathrm{H}^+_{(\mathrm{aqu.})} \Rightarrow n \equiv \mathrm{Si-OH} + \mathrm{M}^{n+}_{(\mathrm{aqu.})} \quad (3)$$

For longer corrosion times, dissolution of the hydrated network is rate-controlling,[13] as schematically shown in the reaction:

$$\equiv \mathrm{Si-O-SiO}_{3-n}(\mathrm{OH})_n + \mathrm{H}^+_{(\mathrm{aqu.})}$$

$$\Rightarrow \mathrm{Si-OH} + \mathrm{SiO}_{3-n}(\mathrm{OH})_{n+1(\mathrm{aqu.})} \quad (4)$$

In corroded glasses the partially hydrated layer is not very stable and can be removed by ultrasonic treatments. This low stability is also the reason why periodic ultrasonic treatment of the oxide nitride glass increases the corrosion rate of the oxide nitride glasses (see Fig. 4). In the corroded Si_3N_4 ceramics this partially hydrated layer is stabilised by the strong Si_3N_4 skeleton. Therefore the corrosion of the Si_3N_4 ceramics YAl 1 can be described by the corrosion behaviour of the GLAY 6 determined under conditions without ultrasonic treatment. The stabilisation of the partially hydrated network layer formed by the dissolution of the amorphous grain boundary phase by the strong skeleton of the Si_3N_4 grains is caused on the one hand by the reduced diffusion of $SiO_2 \times nH_2O$, on the other hand, a reduced destruction of the glass network can be expected by an accelerated condensation reaction in the corrosion layer:

$$2 \equiv \mathrm{Si-O-H} \Rightarrow \equiv \mathrm{Si-O-Si} \equiv + \mathrm{H_2O} \quad (5)$$

reducing the solubility of the partial hydrated network by dehydratisation. This reaction is well known on hydrated silica surfaces and is the reaction converting soluble silicic acid to insoluble silica. This condensation reaction reduces the further destruction of the network and the leaching of the network modifiers. Therefore, the corrosion rate of the ceramics rapidly decreases with increasing corrosion depth. This process of formation of a stable passivating SiO_2 network in the ceramics is strongly accelerated by an increasing amount of SiO_2 in the grain boundary of the ceramics (see Fig. 5). MgO containing glasses show a similar behaviour like the Y_2O_3 containing glasses with the same amount of non-bridging oxygen in the glass network.[13,15]

Additionally, this passivating layer forms more rapidly when the size of the triple junctions is smaller, i.e. when the additive content is lower. The same results can be observed if the size of the triple junctions is reduced without changes in the volume of the grain boundary phase. Additionally the corrosion temperature, concentration and type of the acid will alter this process.[6] This mechanism also seems to be the reason for the high stability of silicon nitride ceramics in concentrated acids.[1–4] Recently microanalysis of the corroded layers showed a gradient in the concentration of the oxygen content, indicating the formation of such layers.[14] Also, oxidation prior to corrosion increases the corrosion resistance drastically and can be explained by this model. The assumption of the formation of a stable hydrated SiO_2-rich network is also in agreement with the different corrosion behaviours in HF and under hydrothermal conditions. First XPS (X-ray photoelectron spectroscopy) investigations of the surface of YAl 1 ceramics which were previously corroded in 2 N H_2SO_4 confirm the formation of a SiO_2 layer and support the assumptions. Further results are underway.

Under hydrothermal conditions, SiO_2-rich glasses are less stable than alumosilicate glasses are. Therefore, the thin films also dissolve and, as a consequence, the corroded layer is unstable under hydrothermal conditions (see Fig. 12a and b). Additionally, the grains start to dissolve at about 180–200 °C in H_2O. This is connected with the higher solubility of SiO_2 under these conditions, leading to a reduction in the stability of the SiO_2 surface layers and protecting the Si_3N_4 particles from undergoing hydrolysis. This altered stability of grains and thin films results in linear corrosion kinetics; i.e. the formation of protective layers is not observed. The corrosion rate for materials with a SiO_2-rich grain boundary is high. Fig. 12a shows that even additive-free HIPSN with only about 3 wt.% SiO_2 in the grain boundaries has a much higher corrosion rate than Y_2O_3/Al_2O_3-containing materials do. The MgO-containing materials Mg Al 1–3 have a similarly high corrosion rate as the HIPSN. This is in agreement with the literature.[1–3,6,11]

Whereas the dissolution rates of the grains and the grain boundary for the YAl 1 material at 210 °C are similar, the grain boundary phase in materials MgAl 1–3 dissolves much faster than the grains, causing a very weak corrosion layer to be formed.

Earlier investigations[1] of Si_3N_4 ceramics with Y_2O_3 and Al_2O_3 as sintering additives indicated that at 250 °C, the dissolution rate of the Si_3N_4 grains was even higher than that of the grain boundary phase, whereas at 180 °C, no pronounced attack was found. This is in agreement with the data observed here.

5. Conclusions

The stability of silicon nitride materials in acids and bases and under hydrothermal conditions strongly depends on the amount and composition of the grain boundary phase.

Silicon nitride materials with a high SiO_2 content in the grain boundary phase are more stable in acids and less stable in bases and under hydrothermal conditions. Materials with a low SiO_2 content in the grain boundary phase are more stable in bases and under hydrothermal conditions and less stable in acids.

This behaviour is more pronounced in materials with a higher amount of grain boundary phase.

The investigations showed that the grains and the thin films between the grains are very stable in acids and bases up at least to 130 °C. This results in strong corrosion layers which influences the kinetics of corrosion and results in a relatively high residual strength, even for a high corrosion depth.

The corrosion behaviour of the investigated materials with a relatively stable grain boundary phase in acids can be described by the same kinetic laws as those used to describe the corrosion of glasses. An interfacial reaction is assumed to be rate-controlling. The less stable material with Y_2O_3/Al_2O_3 additives can be described by the corrosion behaviour of oxide nitride glasses only at the beginning. For higher corrosion depths, the formation of protective barriers consisting of a hydrated SiO_2 network is assumed to occur.

The results of our investigations indicate that tailoring of the microstructure and the grain boundary composition of silicon nitride ceramics is necessary if these materials are to be applied in corrosive environments.

By changing the composition of the material, the corrosion resistance (weight loss and thickness of the corrosion layer) can be changed by more than two orders of magnitude and the reduction of strength minimised.

Acknowledgements

This study was supported by the DFG under contract number HE 2471/1.

References

1. Herrmann, M., Klemm, H. and Schubert, C., Silicon nitride based hard materials. In *Handbook of Ceramic Hard Materials*, ed. R. Riedel. Wiley-VCH, Weinheim, 2000, pp. 747.
2. Komeya, K., Meguro, T., Atago, S., Lin, C. H., Abe, Y. and Komatsu, M., Corrosion resistance of silicon nitride ceramics. In *The Science of Engineering Ceramics II. Key Eng. Mat. 161–163*, ed. K. Niihara, T. Sekino, E. Yasuda and T. Sasa. Trans Tech Publications, Switzerland, 1999, pp. 235.
3. Okada, A. and Yoshimura, M., Mechanical degradation of silicon nitride ceramics in corrosive solutions of boiling sulphuric acid. *Key Eng. Mat.*, 1996, **113**, 227–236.
4. Monteferde, F., Mingazzini, C., Giorgi, M. and Bellosi, A., Corrosion of silicon nitride in sulphuric acid aqueous solution. *Corrosion Science*, 2001, **43**, 1851–1863.
5. White, W. B., Theory of corrosion of glass and ceramics. In *Corrosion of Glass, Ceramics and Ceramic Superconductors*, ed. D. E. Clark and B. K. Zoitos. Noyes Publications, USA, 1992.
6. Herrmann, M., Schubert, C. and Michael, G., Korrosionsstabile keramische Werkstoffe für Anwendungen in Wälzlagern und im Anlagenbau. *cfi DKG Berichte*, 1999, **14**, 130.
7. Schilm, J., Herrmann, M., Michael, G., Kinetic study of corrosion of silicon nitride materials in acids. *J. Eur. Cer. Soc.*, 2003, **23**, 577–584.
8. Wray, P. J., The geometry of two phase aggregates in which the shape of the second phase is determined by its dihidral angle. *Acta Met.*, 1976, **24**, 125.
9. Bando, Y., Mitomo, M. and Kurashima, K. J., An inhomogeneous Grain Boundary Composition in Silicon Nitride. *Mater. Synthesis and Processing*, 1998, **6**, 359.
10. Bobeth, M., Clarke, D. R. and Pompe, W., *J. Am. Ceram. Soc.*, 1999, **82**, 1537.
11. Herrmann, M. and Michael, G., Corrosion behaviour of engineering ceramics in acids and basic solutions. *Br. Ceram. Proc.*, 1999, **60**, 455.
12. Wötting, G., Herrmann, M., Michael, G., Siegel, S., Frassek, L., *Sinteradditive und SiO_2-enthaltende Siliciumnitridwerkstoffe, ein Verfahren zur Herstellung und deren Verwendung*; patent DE 197 46 008.9 (1997) ; WO 99/20579 (1999) patent.
13. Paul, A., Chemical Durability of glasses; a thermodynamic approach. *J. Mater. Sci.*, 1977, **12**, 2246–2268.
14. Seipel, B., Nickel, K.G., *J. Eur. Cer. Soc.* (submitted for publication).
15. Herrmann, M., Schilm, J., Michael, G., *Report of the DFG project* (contract number HE 2471/1).